Biomaterials Science

Tumor extracellular acidity activated "off-on" release of bortezomib from a biocompatible dendrimer

SCHOLARONE™
Manuscripts

Journal Name

ARTICLE

Tumor extracellular acidity activated "off-on" release of bortezomib from a biocompatible dendrimer

Mingming Wang[1a], Yu Wang[2a], Ke Hu[3,4a], Naimin Shao[1] and Yiyun Cheng[1*]

Nanoparticle with specific response to tumor extracellular acidity provides a new option in the design of tumor-targeted delivery systems. In this study, we report such a pH-responsive polymer which realizes "off-on" release of bortezomib at tumor acidic microenvironments. A dendrimer surface is grafted with a neutral shell to reduce its cellular uptake, and its interior is functionalized with catechol moieties. An anticancer drug bortezomib is loaded within the dendrimer interior via boronate-catechol interaction. The bortezomib-loaded dendrimer is non-toxic to a list of cells at physiological conditions, but kills most of the cells at slightly acidic microenvironments. *In vivo* studies further prove that the bortezomib-loaded dendrimer significantly inhibits tumor growth while causing minimal systemic toxicity to the animals. Since there is a list of potent anticancer drugs containing the boronate structure, the polymeric vector in this study provides a versatile scaffold to design pH-responsive drug carriers for chemotherapy.

Introduction

Aerobic glycolysis is a recognized hallmark of malignant tumor.[1] The up-regulated glycolysis and reduced use of oxidative phosphorylation in tumors (also termed the Warburg effect) lead to a high level of secreted lactic acid in the microenvironment.[2] As a result, most of the tumors exhibit a more acidic extracellular microenvironment (pHe 6.5-6.8) compared to normal tissues (pHe 7.2-7.4).[1, 3] The tumor extracellular acidity is ubiquitous in solid tumors, regardless of cancer type, thus it can serve as a general biomarker to design tumor-targeted delivery systems.[1] Compared with traditional cancer-specific biomarkers such as EGFR, Her/neu and PSMA, tumor extracellular acidity mediated cancer targeting is insensitive to protein heterogeneity and is not limited by the number of biomarkers on the cancer cells.[4, 5] Recently, the tumor extracellular acidity is widely used as a stimulus in the design of stimuli-responsive drug delivery systems for cancer treatment. For example, tumor extracellular acidity activates the cellular uptake of charge-reversal materials.[6-9] Alternatively, tumor acidity activates cell penetrating peptides such as transactivator of transcription (TAT) peptide, melittin peptide, and pH (low) insertion peptide (pHLIP), which are linked to a drug or gene vector.[10-13] In most cases, the tumor acidity breaks an acid-sensitive bond in polymeric micelles or capsules, followed by demicellization/degradation and rapid release of entrapped anticancer drugs.[14-19] These tumor acidity-responsive materials increase therapeutic effect and reduce adverse effects of several anticancer drugs.

Bortezomib (BTZ) is a potent and specific proteasome inhibitor for cancer therapy.[20] This compound is now marketed as Velcade which is approval for the treatment of multiple myeloma.[21] However, BTZ is less active against solid tumors, even for myeloma, only 40% of the patients respond to BTZ

when used as a single agent. Systemic administration of BTZ leads to a higher risk of adverse effects such as peripheral neuropathy, thrombocytopenia and cardiotoxicity.[22] In addition, BTZ resistance has been observed in many patients during cancer therapy.[23] These problems are emerging as great challenges in the clinical applications of BTZ. To extend the therapeutic window for BTZ, multiple drug carriers were designed for the delivery of BTZ to cancer cells,[21, 24-26] among which pH-responsive carriers are one of the most promising options.[27] The boronic acid group in BTZ is able to react with polyhydroxyl compounds, forming a boronate ester bond in aqueous solutions.[28, 29] Stability of the boronate ester bond depends on solution acidity.[30] Among the polyhydroxyl compounds, catechol (Cat) shows the highest affinity with boronic acids. The catechol-boronate interaction was adopted to design pH-responsive micelles for the delivery of BTZ and other anticancer drugs.[27, 28] However, these polymeric micelles fail to exhibit an "off-on" drug release behavior (e.g. toxic to cells at physiological conditions) due to the instability of micelles.

In this study, we report a pH-responsive polymer which realizes "off-on" release of BTZ at slightly acidic tumor microenvironments based on a poly(amidoamine) dendrimer. Dendrimers are a class of synthetic polymers with unique properties such as highly symmetrical, monodisperse, well-defined molecular weight and size and high density of surface functionality.[31-33] These polymers are widely used as scaffolds in the design of multifunctional drug and gene carriers.[34-41] Unlike polymeric micelles, dendrimer has excellent stability in diluted solutions and will not disassemble during blood circulation. To avoid the triggered release of anticancer drugs by acidic vesicles (such as endosomes and lysosomes) in normal cells, the dendrimer surface is fully grafted with a neutral shell (acetylated lysine, KAc) to reduce its cellular

uptake (Scheme 1). The dendrimer interior is functionalized with catechol groups to bind BTZ through catechol-boronate interactions. The catechol-boronate interactions in combination with hydrophobic interactions between BTZ and dendrimer hydrophobic interior ensure good stability of the BTZ nanoformulation. These properties together allow the drug carrier to keep its cargos in normal tissues and rapidly release them in tumor acidic microenvironments. The aim of this study is to design a tumor acidity-responsive drug carrier for the delivery of boronic acid containing drugs such as BTZ.

Experimental

Materials

Ethylenediamine (EDA)-cored and amine-terminated generation 5 (G5) poly(amidoamine) dendrimer (stored in methanol) was purchased from Dendritech (Midland, MI). Tetramethylrhodamine isothiocyanate (TRITC), phalloidin-FITC, Hoechst 33342, trifluoroacetic acid (TFA) and deuterated reagents including deuterated water (D_2O) and deuterated dimethyl sulfoxide (d_6-DMSO) were purchased from Sigma-Aldrich (St. Louis, MO). Catechol-4-acetic acid, N-hydroxysuccinimide (NHS), N, N'-dicyclohexylcarbodiimide (DCC) and dichloromethane were purchased from Aladdin (Shanghai, China). N,N-dimethyl formamide (DMF), dimethyl sulfoxide (DMSO) and triethylamine (TEA) were purchased from Sinopharm Chemical Reagent Co., Ltd. (Shanghai, China). Boc-Lys(Ac)-OH was purchased from GL Biochem (Shanghai, China). BTZ was purchased from Yeexin Biochem&Tech (Shanghai, China). AO (acridine orange) was purchased from Sango Biotech (Shanghai, China). EB (ethidium bromide) was purchased from TIANGEN BIOTECH (BEIJING) Co., Ltd (Beijing, China). G5 dendrimer was distilled to remove the methanol before use. The dendrimer was characterized by polyacrylamide gel electrophoresis and 13C NMR to confirm its purity. All the other chemicals were used as received without further purification.

Synthesis of acetylated lysine-modified G5 dendrimer (G5-KAc-NH$_2$).

Boc-Lys(Ac)-OH (499.3 mg, 1.7 mmol) was activated by DCC and NHS (1.95 and 1.8 molar equivalents of Boc-Lys(Ac)-OH, respectively) in 8 mL dehydrated DMF for 6 h. TEA was added as a deacid reagent. Then, G5 dendrimer (300 mg, 10.4 µmol) dissolved in dehydrated DMSO (8 mL) was slowly added into the above solution. The mixture was stirred at room temperature for 7 d. After that, the product was dialyzed against DMSO and lyophilized as white gels. The gels were re-dissolved in a TFA-dichloromethane solution (5 mL, 4:1, v/v) to remove the protecting group. The solvent was distilled and the product was further dialyzed intensively against DMSO and distilled water. The product G5-KAc-NH$_2$ was lyophilized as white gels and characterized by ^{1}H NMR (699.804 MHz, Varian) to determine the number of acetylated lysine groups conjugated on each G5 dendrimer.

Partially (50%) acetylated G5 dendrimer (G5-Ac) was synthesized according to the following procedure. G5

dendrimer (50 mg, 1.7 µmol) was dissolved in anhydrous methanol (2 mL) and added with acetic anhydride (0.1 mmol). TEA was added as a deacid reagent (18.6 µL). The mixture was stirred at room temperature for 24 h and the product was dialyzed intensively against PBS buffer (pH=7.4) and distilled water. The purified product G5-Ac was lyophilized as white gels and characterized by ^{1}H NMR (699.804 MHz, Varian) to determine the number of acetyl groups on each G5 dendrimer.

Synthesis of catechol-conjugated G5-KAc-NH$_2$ (G5-KAc-Cat).

Generally, catechol-4-acetic acid (37.6 mg, 0.2 mmol) was activated by DCC and NHS (1.95 and 1.8 molar equivalents of catechol-4-acetic acid, respectively) in 5 mL dehydrated DMF for 6 h. TEA was added as a deacid reagent (70.1 µL). G5-KAc-NH$_2$ (350.0 mg, 7.0 µmol) dissolved in 5 mL dehydrated DMSO was slowly added into the above solution. The product G5-KAc-Cat was dialyzed intensively against DMSO and distilled water, and lyophilized as white powders. The number of catechol groups conjugated on each G5 dendrimer is determined by ^{1}H NMR (699.804 MHz, Varian).

Catechol-conjugated G5 and G5-Ac dendrimers were synthesized according to the same method (the molar ratio of catechol-4-acetic acid and dendrimer is 32:1). TRITC-labeled G5 dendrimer and G5-KAc-Cat were synthesized by mixing G5 dendrimer (20 mg, 0.7 µmol) or G5-KAc-Cat (20 mg, 0.4 µmol) with TRITC (the molar ratio TRITC and dendrimer is 2:1) in 2 mL distilled water for 24 h. The product was purified by intensive dialysis against distilled water and lyophilized before use. Fluorescence spectra of the TRITC-labeled polymers were taken by a fluorescence spectrophotometer (F-4500, Hitachi).

Preparation of BTZ-loaded G5-KAc-Cat.

BTZ was dissolved in DMSO at a concentration of 260.3 mM. G5-KAc-Cat was dissolved in distilled water (181.7 µM). Then BTZ was added into the G5-KAc-Cat solution at a BTZ/G5-KAc-Cat molar ratio of 10:1. The mixture was maintained at 37 °C for 2 h before *in vitro* and *in vivo* experiments. BTZ-loaded G5-KAc-NH$_2$ was prepared as a control.

[1]H-^{1}H nuclear Overhauser effect spectroscopy(NOESY) analysis of BTZ-loaded G5-KAc-Cat.

The BTZ-loaded G5-KAc-Cat complex (72.7 µM G5-KAc-Cat, the molar ratio of BTZ/G5-KAc-Cat is 10:1, pH=7.4) in D_2O/d_6-DMSO (0.5% d_6-DMSO, v/v, d_6-DMSO was added to dissolve BTZ) was analyzed by [1]H-^{1}H NOESY (699.804 MHz, Varian). 10 µg dioxane was added into the complex solution as an internal standard. Generally, the [1]H-^{1}H NOESY experiment was conducted using a standard pulse sequence. A water suppression pulse was added to improve signal sensitivity. 1 s relaxation delay, 146.63 ms acquisition time, a 6.5 µs 90° pulse width, and 32 transients were averaged for 512 × 1024 complex points. The mixing time is 300 ms. All the data were processed with NMRpipe software on a Linux workstation.

***In vitro* release of BTZ from G5-KAc-Cat.**

In vitro drug release was investigated by an equilibrium dialysis method. Generally, BTZ-loaded G5-KAc-Cat complex (3.9 mmol BTZ, the molar ratio of BTZ/G5-KAc-Cat is 10:1) was dialyzed against PBS buffer (pH=7.4) to remove unbound BTZ for 2 h. The purified complexes were immediately transferred into a dialysis bag with a molecular weight cut off of 3500 Da. The dialysis bags were immersed into a container filled with 50 mL PBS buffer (pH condition was adjusted to 7.4, 6.5 and 5.0, respectively). The outer phase of the dialysis bag was stirred at 300 rpm during the *in vitro* release studies. 10 μL of the samples were collected at scheduled time intervals from the outer phase and the BTZ concentration in the collected sample was determined by high-performance liquid chromatography (HPLC, Agilent1200). The HPLC instrument was equipped with a C18 column (4.6 mm diameter, 150 mm length, 5 μm particle size, ZORBAX Eclipse XDB, Agilent, U.S.A.). The mobile phase was methanol and deionized water (70%/30%, v/v) at a flow rate of 1.0 mL/min. 10 μL sample was injected and detected at 260 nm. The standard curve for BTZ was conducted at BTZ concentration range of 0-50 μg/mL ($A=13.8698C-0.5509$, C is the BTZ concentration, μg/mL, A is the peak area $R^2=0.99998$). The release profiles of BTZ from G5-KAc-NH$_2$ and vector-free PBS solution were measured as controls.

Cell culture and cytotoxicity assay.

HeLa (a human cervical carcinoma cell line, ATCC), MCF-7 (a human breast adenocarcinoma cell line, ATCC), MG-63 (a human bone osteosarcoma cell line, ATCC) and NIH3T3 (a mouse embryo fibroblast cell line, ATCC) cells were cultured in DMEM. MDA-MB-231 cells (a human breast adenocarcinoma cell line, ATCC) were cultured in MEM. PC-9 cells (a human lung adenocarcinoma cell line, ATCC) were cultured in RPMI 1640 medium. The cell culture mediums were supplemented with 10% fetal bovine serum (FBS), 100 U/mL streptomycin, and 100 U/mL penicillin. All the cells were cultured at 37 °C under 5% CO$_2$.

The cytotoxicity of BTZ or BTZ complexes on the six cell lines was measured by a well-established 3-(4,5-dimethylthiazol-2-yl)-2, 5-diphenyltrazolium bromide (MTT) assay. The cells were cultured in 96-well plates at a density of 10^4 cells per well. The cells were cultured 48 h before cytotoxicity studies. Then the cells were incubated with BTZ or BTZ complexes (pH values of the complex were adjusted to 7.4, 6.5 and 5.0 before incubation with the cells) for 48 h, followed by wash of cells with fresh PBS and incubation of the cells with MTT containing medium for 2 h. DMSO was further added to the wells to dissolve the yielding purple formazan. Absorbance of the solution in each well was detected at 490 nm by a microplate reader (MQX200R, BioTek Inc.), and the obtained values were used to reflect cytotoxicity of the tested drugs or complexes. Five repeats were conducted for each sample and data were given as means ± S.E.M.

The cytotoxicities of BTZ and BTZ-loaded G5-KAc-Cat on MDA-MB-231, MCF-7 and MG-63 cells were also evaluated by an AO/EB double-staining assay. The incubated cells were stained by AO (5 μg/mL) and EB (5 μg/mL) in PBS for 10 min. The stained cells were washed with PBS and imaged by a fluorescence microscope (Moticam 5000, Motic Instruments Inc.). Cells without any treatment were tested as controls.

Celluar uptake of G5-KAc-Cat and G5 dendrimer.

To analyze the cellar uptake of G5-KAc-Cat and G5 dendrimer, both materials were labeled with a red fluorescent dye TRITC. Generally, HeLa cells were seeded in 24-well plates before incubated with TRITC-labeled polymers (500 nM) at 37 °C for 6 h, 12 h, 24 h and 48 h, respectively. The cells in each well were digested with trypsin, re-suspended in 300 μL PBS and analyzed by flow cytometry. The cellular uptake of the TRITC-labeled G5-KAc-Cat and G5 dendrimer was also observed by a laser scanning confocal microscopy (LSCM, Leica). Before LSCM experiments, the cells were incubated with the TRITC-labeled polymers (500 nM) for 12 h, washed with PBS, and further stained with phalloidin-FITC (5 μg/mL, 20 min) and Hoechst 33342 (5 μg/mL, 10 min). Finally, the cells were washed with PBS for three times and examined by LSCM.

Establishment of tumor model.

MDA-MB-231 cells and PC-9 cells stably expressing luciferase (MDA-MB-231-luc and PC-9-luc) were established by transfecting the cells with plasmid co-expressing the firefly luciferase gene and kanamycin (G418) resistance gene using Lipofectamine 2000 (Invitrogen, Carlsbad, CA). MDA-MB-231-luc cells and PC-9-luc cells were selected by G418 resistance. Bioluminescence activity of the cells in the presence of D-luciferin was examined by Xenogen IVIS-200 (Caliper Life Sciences, Hopkinton, MA). All the animal experiments in this study were carried out according to the National Institutes of Health guidelines for care and use of laboratory animals and approved by the ethics committee of East China Normal University. The animals were housed under specific-pathogen-free conditions within the animal care facility at East China Normal University. Balb/c nude female mice (5-week-old, ~25 g) were used to establish the tumor models. For the subcutaneous tumor model, MDA-MB-231-luc cells (~10^6 cells) suspended in 20 μL PBS were subcutaneously injected into flank of each mouse. For the bone tumor model, PC-9-luc cells (~10^5 cells) suspended in 20 μL PBS were injected into the tibias of mice via a percutaneous approach.

Anticancer activity of BTZ-loaded G5-KAc-Cat complex *in vivo*.

For the subcutaneous MDA-MB-231-luc tumor model, when tumor size reaches about 300 mm^3, the mice were randomly divided into three groups with three mice in each group. The mice were administrated with PBS, BTZ and BTZ-loaded G5-KAc-Cat complex, respectively via intratumoral injection (1 mg

BTZ/kg mice). The treatments were repeated every two days for a total number of three injections. For the bone tumor model, the treatment was initiated at the third week after the establishment of PC-9-luc bone tumor model. The mice were randomly divided into three groups with three mice in each group and administrated with PBS, BTZ and BTZ-loaded G5-KAc-Cat complex, respectively via tail vein injection (0.5 mg BTZ/kg mice). The treatments were repeated every two days for a total number of three injections. The bioluminescence images of tumor in each mouse were measured using Xenogen IVIS-200 before and after the treatments, respectively. The body weights of mice were recorded every two days. The results were analyzed by student's t-test.

TUNEL assay.

The mice bearing MDA-MB-231-luc tumors after treatment were sacrificed. The fresh tumor tissues harvested from the sacrificed mice were fixed in 4% formalin solution, embedded in paraffin, and sectioned into slices with a thickness of 4 μm. The tumor sections were then incubated with proteinase K, TUNEL reaction mixture and Hoechst 33342 according to the protocols of in situ apoptosis detection kit (Roche, Mannheim Germany). Apoptotic cells in the sections were imaged by a fluorescence microscope.

Blood toxicity assay.

BALB/c mice (~18 g) were randomly divided into three groups with five mice in each group. The mice were administrated with PBS, BTZ and BTZ-loaded G5-KAc-Cat complex, respectively via intraperitoneal injection. The treatments were repeated every two days for four injections and the dose for each injection was 0.5 mg, 0.5 mg, 0.75 mg and 1 mg BTZ/kg mice, respectively. The body weight of mice was recorded every two days. The mice were sacrificed two days after the last treatment and the blood from each mouse were collected for blood toxicity assay using a hematology analyzer (HEMAVET-950, Drew Scientific Inc.).

Results and discussion

Synthesis and characterization of G5-KAc-Cat and BTZ-loaded G5-KAc-Cat complex

As shown in Scheme 1, the surface of G5 dendrimer was grafted with acetylated lysine via a facile condensation reaction. According to the ^{1}H NMR spectrum in Fig. 1a, an average number of 125 acetylated lysine molecules are conjugated on G5 dendrimer surface, suggesting that the dendrimer surface is fully grafted with the acetylated amino acid (a theoretical number of 128 primary amine groups on each G5 dendrimer). Replacement of the cationic amine groups on G5 dendrimer with acetylated lysine can efficiently decrease cellular uptake as well as cytotoxicity of the cationic dendrimer. The yielding G5-KAc-NH$_2$ was further reacted with catechol-4-acetic acid (Scheme 1) to yield G5-KAc-Cat. According to the ^{1}H NMR spectrum in Fig. 1b, about 33 catechol groups are functionalized on each G5-KAc-NH$_2$. In comparison, G5 and partially acetylated G5 (G5-Ac) dendrimers yield insoluble

dendrimer-catechol conjugates when reacted with catechol-4-acetic acid. This is because the acetylated lysine groups on G5-KAc-NH$_2$ provide a more hydrophilic surface, shielding the conjugated catechol groups from dendrimer surface. Such a strategy efficiently improves the stability of dendrimer-catechol conjugates.
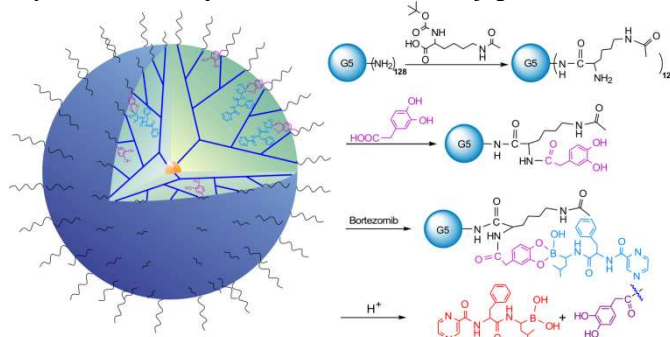
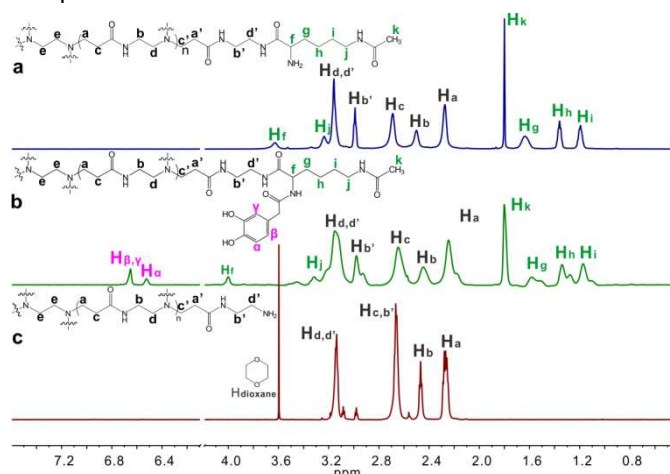**Scheme 1** Synthesis of G5-KAc-Cat and the pH-responsive mechanism of BTZ-loaded G5-KAc-Cat complex.

Fig. 1 ^{1}H NMR spectra of G5-KAc-NH$_2$ (a), G5-KAc-Cat (b) and unmodified G5 poly(amidoamine) dendrimer (c) in D$_2$O.

When BTZ was added into G5-KAc-Cat, it forms a stable complex with the vector via the catechol-boronate interactions. The average size of BTZ-loaded G5-KAc-Cat is measured to be 6.6 nm by dynamic light scattering. We further use a ^{1}H-^{1}H NOESY technique to reveal the complex structure of BTZ-loaded G5-KAc-Cat. ^{1}H-^{1}H NOESY is capable of revealing spatial relationships among protons in a complex.[42] It is widely used to prove host-guest interactions in inclusion complexes.[43] Generally, if two protons in a complex are in close proximity to each other (within 5 Å), cross-peak between them appears in the NOE spectroscopy. As shown in Fig. 2, strong NOE cross-peaks between the methylene protons (H$_{a-d}$) of G5 dendrimer and aromatic protons (H$_{\alpha, \beta, \gamma}$) of catechol are observed. These protons are in close proximity with each other in the BTZ-loaded G5-KAc-Cat complex. Since protons Hb, d on G5 poly(amidoamine) dendrimer are closer to the dendrimer surface than protons Ha, c localized in dendrimer interior, the stronger intensities for cross-peaks between protons H$_{a, c}$ and H$_{\alpha, \beta, \gamma}$ in Fig. 2 indicates that catechol groups are entrapped in the hydrophobic dendrimer interior. Similarly, strong NOE cross-peaks are observed between protons (H$_{4-8, 13}$) on BTZ and Ha-d on G5 dendrimer. According to the cross-peaks, both aromatic rings and methyl groups of BTZ localize in the dendrimer interior, suggesting that hydrophobic interaction plays an important role in the formation of

BTZ/G5-KAc-Cat complex. Taken together, the ^1H-^1H NOESY prove that both BTZ and catechol are entrapped in dendrimer interior pockets rather than on dendrimer surface in the complex.
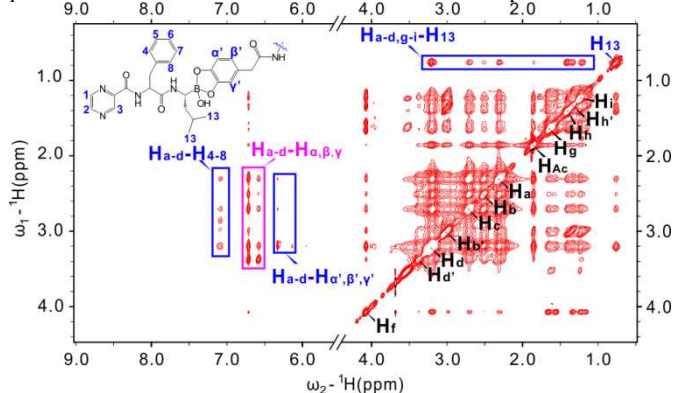

Fig. 2 ^1H-^1H NOESY spectrum of BTZ-loaded G5-KAc-Cat complex at pH 7.4. The mixing time is 300 ms. BTZ and G5-KAc-Cat molar ratio is 10:1.
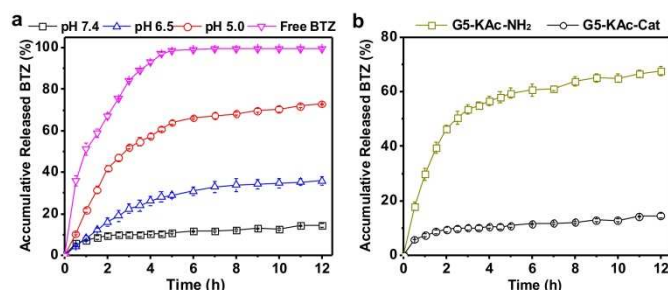

Fig. 3 *In vitro* release profiles of BTZ from the complexes. (a) *In vitro* release of BTZ from G5-KAc-Cat at different pH 7.4, 6.5 and 5.0. Free BTZ in the absence of polymeric vector is tested as a control. (b) *In vitro* release of BTZ from G5-KAc-Cat and G5-KAc-NH$_2$ at pH 7.4. The molar ratio of BTZ and polymeric vector is fixed at 10:1.

pH-triggered release of BTZ from G5-KAc-Cat

We further investigate the *in vitro* release profiles of BTZ from the complex at different pH conditions. As shown in Fig. 3a, nearly 100% of the BTZ molecules release out of the dialysis bag within 4 h in the absence of drug carrier. In comparison, a small percent of the released drug was detected at 12 h in the presence of G5-KAc-Cat at pH 7.4. The slow release of BTZ from G5-KAc-Cat indicates that BTZ-loaded G5-KAc-Cat is stable at physiological conditions. At acidic conditions (pH 6.5 and pH 5.0, to mimic the tumor extracellular acidity and lysosomal acidity, respectively), BTZ exhibits much faster release profiles from the complex, suggesting the pH-responsive behavior of boronate ester bond in the complex. As demonstrated in the references, tumor extracellular microenvironment has a pH value of 6.5-6.8.[1] The faster release of BTZ from G5-KAc-Cat at pH 6.5 further proves that the prepared complex can be activated by tumor extracellular acidity. As shown in Fig. S1, the release of BTZ from the vector can be triggered by changing pH value of the receptor solution from 7.4 to 6.5 or 5.0. To confirm the catechol in G5-KAc-Cat plays an essential role in binding BTZ, we also investigated the release of BTZ from G5-KAc-NH$_2$. As shown in Fig. 3b, BTZ rapidly release from G5-KAc-NH$_2$ in PBS, which is much faster than that from G5-KAc-Cat at pH 7.4.

Though dendrimer/drug complexes are able to retard the release of hydrophobic drugs in water, burst release still occurs in PBS if the drugs are loaded via non-covalent interactions.[44] The presence of catechol groups significantly retards the release of BTZ from the vector.

To characterize the pH-responsive behavior of BTZ-loaded G5-KAc-Cat complex, we analyzed ^1H NMR spectra of the complex at pH 7.4 and 5.0. As shown in Fig. 4a, peaks for methyl protons (H$_{13}$) and aromatic protons (H$_{4-8}$) on BTZ appear in the range of 0.6 ppm and 7.0-7.2 ppm, respectively. After complexation with G5-KAc-Cat, these peaks become broaden, suggesting the formation of stable complex with the large molecular weight polymer. The disappearance of sharp peak for H$_{13}$ in the BTZ/G5-KAc-Cat complex at pH 7.4 suggests that most of the BTZ molecules are in bound-state in the complex (Fig. 4b). When pH of the complex solution was adjusted to 5.0 (Fig. 4c), the BTZ peaks shift to their original positions (free BTZ), demonstrating that most of the BTZ molecules are in free-state in the complex at pH 5.0. These results further prove that BTZ/G5-KAc-Cat is pH-responsive and well explains the *in vitro* release behaviors of BTZ from the complex.
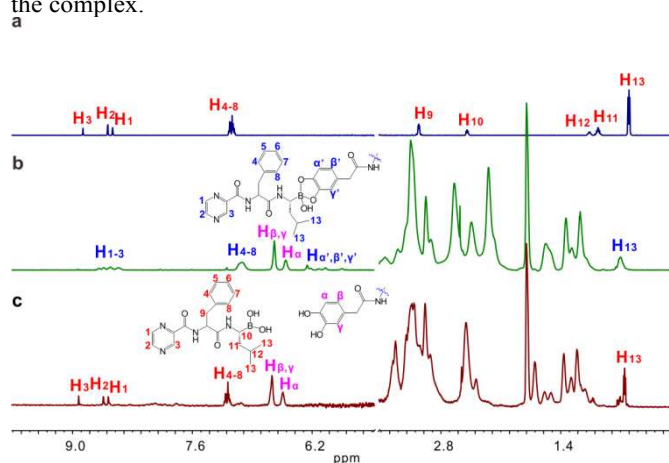

Fig. 4 ^1H NMR spectra of free BTZ (a) and BTZ-loaded G5-KAc-Cat complex at pH 7.4 (b) or pH 5.0 (c).
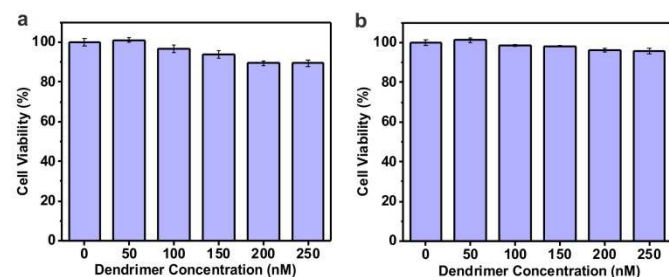

Fig. 5 *In vitro* cytotoxicity of G5-KAc-Cat on (a) NIH3T3 and (b) HeLa cells for 48 h.

Anticancer activity of BTZ-loaded G5-KAc-Cat *in vitro*.

The pH-responsive behavior of BTZ-loaded G5-KAc-Cat was further confirmed on cells. As shown in Fig. 5, the vector G5-KAc-Cat causes minimal toxicity to NIH3T3 and HeLa cells. 90% of the cells survive when incubated with the vector (up to 250 nM) for 48 h, suggesting that G5-KAc-Cat has low cytotoxicity. The low cytotoxicity of G5-KAc-Cat is attributed to its acetylated surface.[45] Cytotoxicity of BTZ-loaded G5-KAc-Cat was further evaluated on six cell lines including

HeLa, MCF-7, MDA-MB-231, PC-9, MG-63 and NIH3T3 (Fig. 6). The complex at neutral pH (BTZ-loaded G5-KAc-Cat at pH 7.4, BTZ/vector molar ratio is 10:1) shows minimal toxicity to all the cells (BTZ half-maximal inhibitory concentration $IC_{50} > 1000$ nM), suggesting excellent stability of the BTZ/G5-KAc-Cat complex at physiological conditions. In comparison, the complex in acidic solutions (pH 6.5 and 5.0) shows significant toxicity to the six cell lines. IC_{50} values of the complex at pH 5.0 on these cells approach that of free BTZ (Table 1). Even at pH 6.5, the complex shows significant toxicity to the cancer cells. The BTZ/G5-KAc-Cat complex prepared at higher BTZ feeding ratio (BTZ/vector molar ratio of 20:1) also shows significant pH-responsive behavior on PC-9 cells (Fig. S2). The pH-responsive toxicity of BTZ/G5-KAc-

Cat complex on MDA-MB-231 cells was further proved by an AO/EB double-staining assay. AO is able to stain normal and necrotic cells, while EB is only taken by necrotic cells with damaged membranes, resulting in bright green and orange fluorescence on normal and necrotic cells, respectively. As shown in Fig. 7, BTZ/G5-KAc-Cat (200 nM BTZ, BTZ/vector molar ratio is 10:1) at pH 7.4 does not cause obvious toxicity to MDA-MB-231 cells, while the complex at pH 6.5 as well as free BTZ can effectively kill the cancer cells (MCF-7 and MG-63 cells in Fig. S3). These results together suggest that BTZ/G5-KAc-Cat can realize "off-on" triggered release of BTZ from the drug carrier by tumor extracellular or lysosomal acidity.
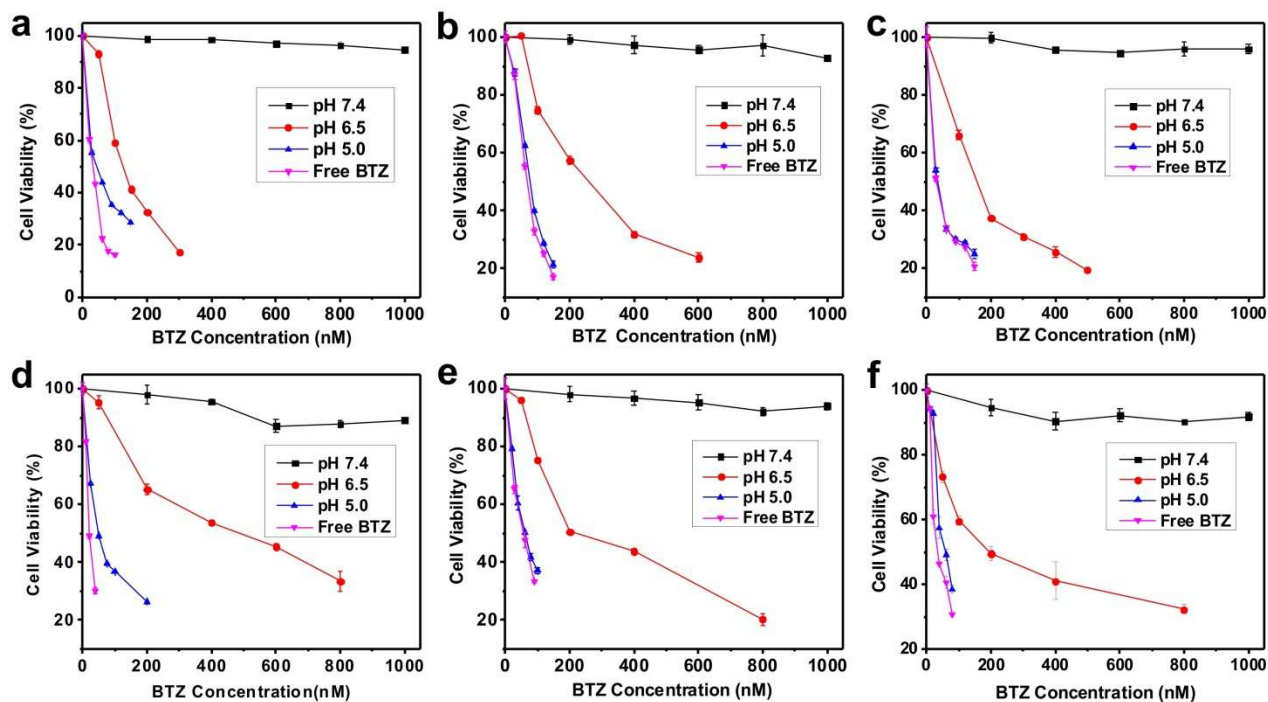

Fig. 6 *In vitro* cytotoxicity of BTZ-loaded G5-KAc-Cat complex (pH 7.4, 6.5 and 5.0) on (a) HeLa (b) MCF-7 (c) MG-63 (d) PC-9 (e) NIH3T3 and (f) MDA-MB-231 cells for 48 h. The molar ratio of BTZ and polymeric vector is 10:1. pH of the complex solution was adjusted to pH 7.4, 6.5 and 5.0 before incubation with the cells. Toxicities of free BTZ on the cells at different molar concentrations were tested as controls.

To prove the essential role of catechol in the complex, we compared the cytotoxicity of BTZ/G5-KAc-NH$_2$ and BTZ/G5-KAc-Cat complexes on NIH3T3, HeLa and MCF-7 cells. As shown in Fig. S4-S6, BTZ/G5-KAc-Cat is non-toxic to the cells at BTZ concentrations up to 1000 nM, in comparison, BTZ/G5-KAc-NH$_2$ show similar cytotoxicity on both cells with free BTZ, indicating that the catechol moieties in the polymer play

Table 1 IC_{50} values of BTZ and BTZ-loaded G5-KAc-Cat (pH 7.4, 6.5 and 5.0).

IC_{50} (nM)	Free BTZ	pH=7.4	pH=6.5	pH=5.0
HeLa	32.6±0.7	N/A	126.7±0.6	45.2±1.4
MCF-7	66.8±0.7	N/A	258.8±3.6	76.4±0.1
MG-63	31.7±0.1	N/A	156.3±0.7	36.3±1.3
PC-9	19.2±0.7	N/A	487.3±2.3	47.9±0.6
NIH3T3	55.2±1.2	N/A	216.8±0.6	61.6±2.7
MDA-MB-231	35.3±1.3	N/A	194.2±2.0	57.9±4.2

an essential role in binding/releasing BTZ.

If BTZ/G5-KAc-Cat complex is internalized by cells, the BTZ release may also be triggered by lysosomal acidity. In this case, the complex will cause cytotoxicity to normal cells, such as NIH3T3 cells. However, as revealed in Fig. 6, the complex is non-toxic to all the cells at pH 7.4, suggesting that the complex is not efficiently internalized by the cells. To confirm this point, we compared the cellular uptake efficiency of G5 and G5-KAc-Cat. Both dendrimers were labeled with a red fluorescence dye-TRITC (Fig. S7). As shown in Fig. 8a, G5-KAc-Cat exhibits extremely low cellular uptake even when incubated with the cells for 48 h. In comparison, cationic G5 dendrimer shows a time-dependent uptake profile (100% cellular uptake) by HeLa cells. The confocal images in Fig. 8b also confirm that G5-KAc-Cat has much lower cellular uptake efficiency than G5 dendrimer. The low cellular uptake efficiency of G5-KAc-Cat is due to the neutral shell (acetylated lysine) grafted on G5 dendrimer (G5-KAc-Cat, +5 mV).
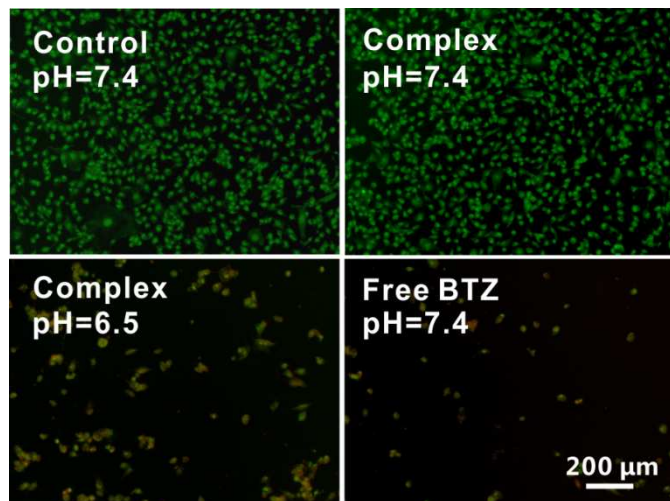
Fig. 7 AO/EB-stained MDA-MB-231 cells after incubated with BTZ-loaded G5-KAc-Cat complex at different pH conditions (200 nM BTZ, the molar ratio of BTZ and polymeric vector is 10:1). pH of the complex solution was adjusted to pH 7.4 and 6.5 before incubation with the cells. Cells without treatment or treated with free BTZ (200 nM) were tested as controls. The viable cells are observed in bright green fluorescence.
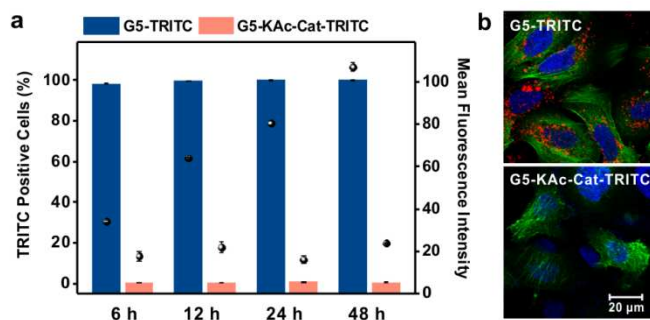

Fig. 8 Cellular uptake of TRITC-labeled G5 dendrimer and G5-KAc-Cat. (a) HeLa cells were incubated with TRITC-labeled G5 dendrimer and G5-KAc-Cat for 6 h, 12 h, 24 h and 48 h, respectively, followed by flow cytometry analysis. Columns represent positive TRITC-labeled cells and black balls represent mean fluorescence intensity (n = 3). (b) Confocal images of HeLa cells treated with TRITC (red)-labeled G5 dendrimer and G5-KAc-Cat for 12 h. The actin filaments were stained with phalloidin-FITC (green) and the nuclei were stained with Hoechst 33342 (blue).

Anticancer activity of BTZ-loaded G5-KAc-Cat *in vivo*.

We further investigate if BTZ-loaded G5-KAc-Cat can be activated by tumor extracellular acidity when the complex is injected into tumors. As shown in Fig. 9a and Fig. 9b, BTZ-loaded G5-KAc-Cat shows similar activity on the inhibition of tumor with free BTZ. Both formulations can significantly inhibit the growth of MDA-MB-231 tumors compared to the control group (treated with PBS). This result clearly demonstrates that tumor extracellular acidity activates the release of BTZ from the biocompatible dendrimer. In addition, administration with free BTZ causes a decrease in body weight, while the complex treatment induces minimal change in body weight compared to the PBS group (Fig. 9c), suggesting a
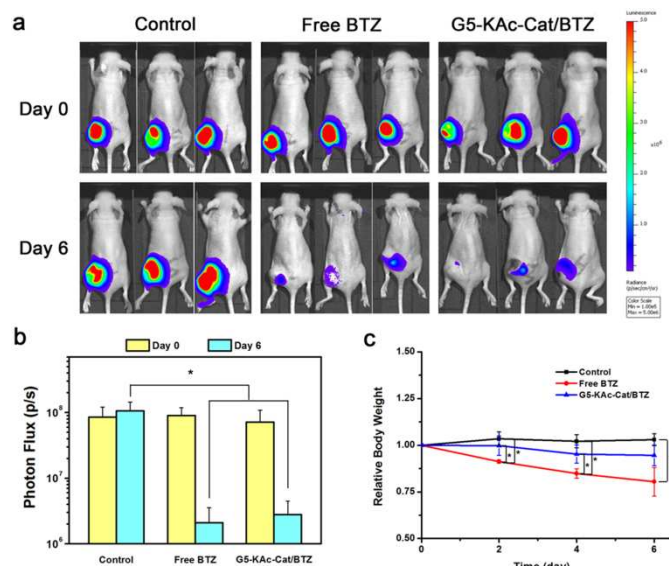

Fig. 9 (a) Bioluminescence images of mice bearing MD-MB-231-Luc tumors treated with PBS, free BTZ and BTZ-loaded G5-KAc-Cat, respectively. (b) Photon flux in the bioluminescence images. (c) Relative body weight of animals bearing MDA-MB-231 tumors during the treatment. Error bars in (b) and (c) represent the s.e. (n=3). *p < 0.05 by students' t-test.
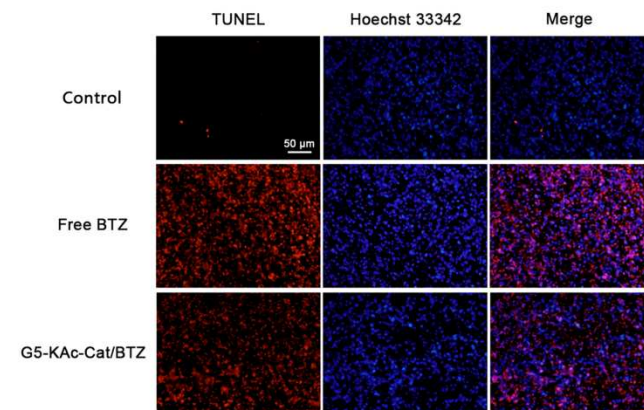

Fig. 10 Apoptosis in tumors of the PBS group, the free BTZ group, and the BTZ-loaded G5-KAc-Cat group analyzed by a TUNEL method (red). The cell nuclei were labeled with Hoechst 33342 (blue).

lower systemic toxicity of BTZ-loaded G5-KAc-Cat. We further examined the apoptosis level in tumors after the animals were treated with BTZ-loaded G5-KAc-Cat by a TUNEL assay. As shown in Fig. 10, much more apoptotic cells are observed in tumor of the complex group compared to that of the PBS group. Similarly, we investigated the anticancer activity of BTZ-loaded G5-KAc-Cat in a bone tumor model by intravenous administration. Bone tumor is a frequent type of cancer that lacks effective clinical treatment. As shown in Fig. S8 and Fig. S9, BTZ-loaded G5-KAc-Cat is more effective on the inhibition of tumor growth than free BTZ. The high anticancer activity of BTZ-loaded G5-KAc-Cat can be explained by the enhanced permeability and retention effect of dendrimer in cancer therapy. In addition, the body weight of animals treated with BTZ-loaded G5-KAc-Cat is similar to the PBS group,

while the free BTZ treated animals show systemic toxicity (Fig. 10). These results together prove that BTZ release can be triggered by tumor extracellular acidity *in vivo* and the BTZ-loaded polymer cause minimal systemic toxicity to the animals.

Pancytopenia is one of the major adverse effects of BTZ in clinical trials. We further compared the systemic toxicities of free BTZ and BTZ-loaded G5-KAc-Cat by blood cell counting. As shown in Fig. 11, the number of white blood cells, lymphocyte, neutrophil, red blood cells, platelet as well as hemoglobin concentration in animals treated with BTZ-loaded G5-KAc-Cat is comparable to those in PBS-treated animals. In comparison, BTZ treatment causes significant decreases in blood cell counts and hemoglobin concentration. The significant blood toxicity of BTZ also causes a decrease in animal body weight (Fig. S11). These results again prove that G5-KAc-Cat is a biocompatible and smart drug carrier for BTZ.
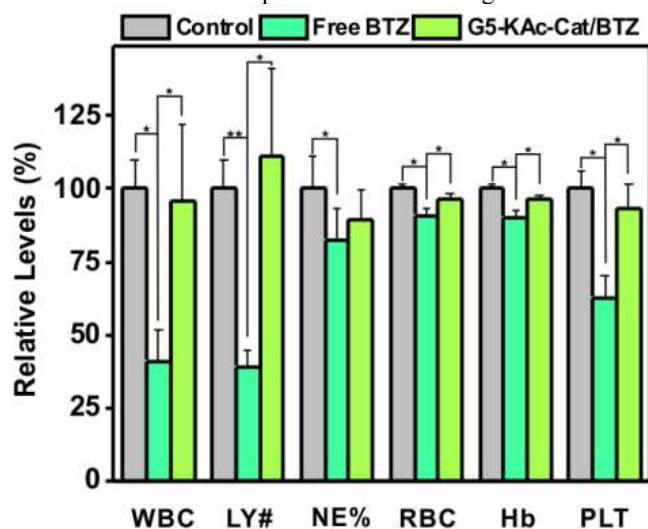

Fig. 11 Analysis of blood samples in normal BALB/c mice treated with PBS (control), free BTZ and BTZ-loaded G5-KAc-Cat, respectively. The white blood cells (WBC), lymphocyte (LY#), neutrophile granulocyte (NE%), red blood cells (RBC), platelet (PLT) and haemoglobin concentration (Hb) in the blood samples were tested by HEMAVET-950. Error bars represent the s.e. (n=5). *$p < 0.05$ and **$p < 0.001$ by students' t-test.

Conclusions

In summary, we present a smart and biocompatible drug vector for boronic acid containing anticancer drugs such as BTZ. Anticancer drug release from the prepared formulation can be activated by tumor extracellular acidity *in vitro* and *in vivo*. The acetylated lysine shell grafted on dendrimer improves the biocompatibility and stability of dendrimer-catechol conjugates, and reduces its non-specific cellular uptake. The catechol moieties conjugated in the dendrimer interior play an essential role in binding and releasing the anticancer drug BTZ. In the BTZ-loaded polymer complex, catechol and BTZ are encapsulated within dendrimer interior via a combination of catechol-boronate interaction and hydrophobic interactions. Due to these unique properties, the BTZ-loaded polymer is non-toxic to six cell lines at physiological conditions, but kills most of the cancer cells with relatively low IC_{50} values at acidic microenvironments. *In vivo* studies also prove that BTZ-loaded polymer can be activated by tumor extracellular acidity.

Administration with BTZ-loaded polymer causes minimal systemic toxicity to the animals. Such a "off-on" triggered release behavior of BTZ-loaded polymer allows maintaining the therapeutic efficacy of BTZ in cancer therapy, while reducing its adverse effects. The current work is limited to "proof-of-concept" experiments, and a long road lies ahead to improve the blood circulation time of the polymer when administrated via intravenous route. We are addressing such limitations by modification of the dendrimer surface with poly(ethylene glycol) chains and targeting moieties. This work will provide a promising therapeutic option for the treatment of cancers.
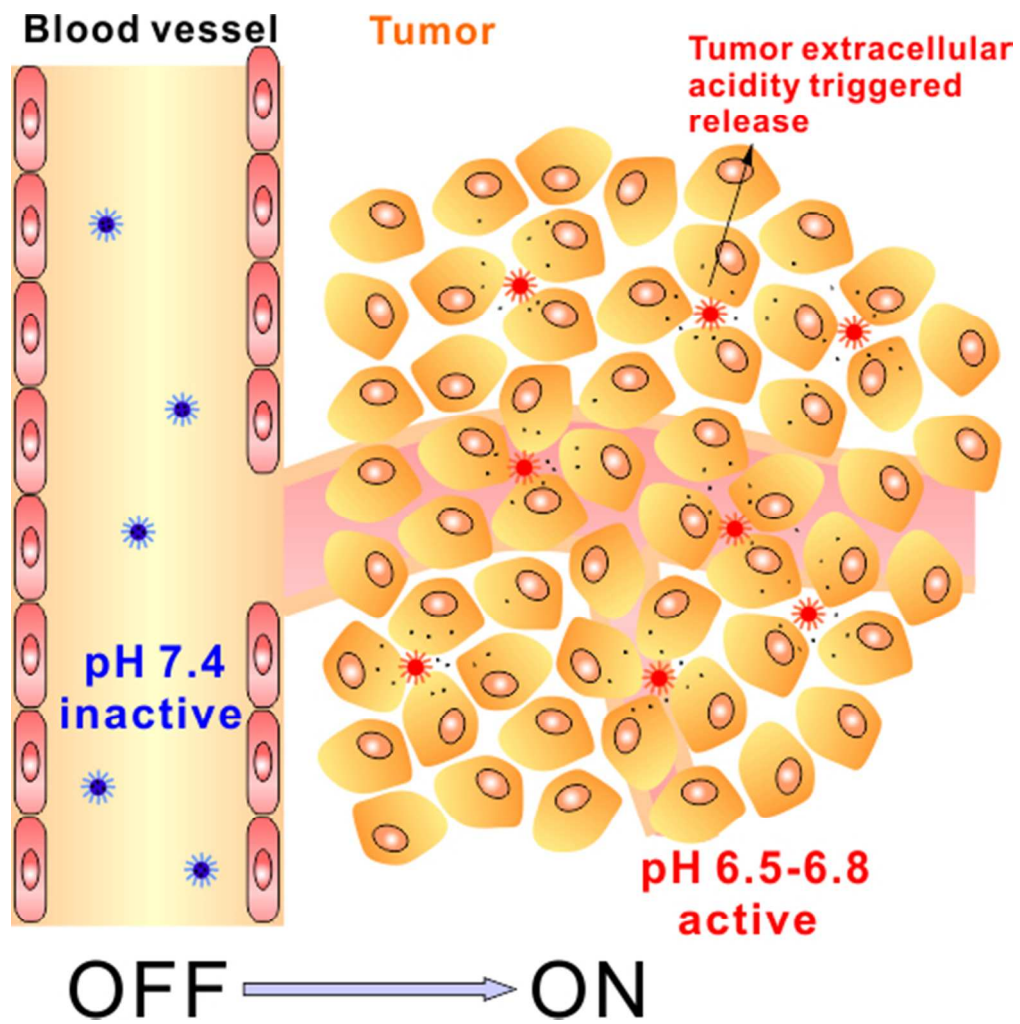
Notes and references

[1]Shanghai Key Laboratory of Regulatory Biology, School of Life Sciences, East China Normal University, Shanghai, 200241, P. R. China

[2]Department of Spine Surgery, First Affiliated Hospital of Wenzhou Medical University, Zhejiang 325000, P.R. China

[3]Department of Gynecology and Obstetrics, Renji Hospital, School of Medicine, Shanghai Jiao Tong University, Shanghai, China

[4]Shanghai Key Laboratory of Gynecologic Oncology, Shanghai, China

[a]These authors contributed equally on this manuscript

[*]Correspondence should be addressed to Y.C. (E-mail: yycheng@mail.ustc.edu.cn)

Electronic Supplementary Information (ESI) available: Further data on the *in vitro* release of drugs from the polymer and the cytotoxicity of drug/polymer complexes. See DOI: 10.1039/b000000x/

1. Y. Wang, K. Zhou, G. Huang, C. Hensley, X. Huang, X. Ma, T. Zhao, B. D. Sumer, R. J. DeBerardinis and J. Gao, Nat. Mater., 2014, 13, 204-212.

2. S. H. Crayton and A. Tsourkas, ACS Nano, 2011, 5, 9592-9601.

3. V. Estrella, T. Chen, M. Lloyd, J. Wojtkowiak, H. H. Cornnell, A. Ibrahim-Hashim, K. Bailey, Y. Balagurunathan, J. M. Rothberg, B. F. Sloane, J. Johnson, R. A. Gatenby and R. J. Gillies, Cancer Res., 2013, 73, 1524-1535.

4. Z. Zhao, H. Meng, N. Wang, M. J. Donovan, T. Fu, M. You, Z. Chen, X. Zhang and W. Tan, Angew. Chem. Int. Ed., 2013, 52, 7487-7491.

5. X. Yu, X. Yang, S. Horte, J. N. Kizhakkedathu and D. E. Brooks, Biomaterials, 2014, 35, 278-286.

6. J. Z. Du, X. J. Du, C. Q. Mao and J. Wang, J. Am. Chem. Soc., 2011, 133, 17560-17563.

7. J. Z. Du, T. M. Sun, W. J. Song, J. Wu and J. Wang, Angew. Chem. Int. Ed., 2010, 49, 3621-3626.

8. D. Ling, W. Park, S. J. Park, Y. Lu, K. S. Kim, M. J. Hackett, B. H. Kim, H. Yim, Y. S. Jeon, K. Na and T. Hyeon, J. Am. Chem. Soc., 2014, 136, 5647-5655.

9. J. Z. Du, C. Q. Mao, Y. Y. Yuan, X. Z. Yang and J. Wang, Biotechnol. Adv., 2014, 32, 789-803.

10. E. Jin, B. Zhang, X. Sun, Z. Zhou, X. Ma, Q. Sun, J. Tang, Y. Shen, E. Van Kirk, W. J. Murdoch and M. Radosz, J. Am. Chem. Soc., 2013, 135, 933-940.

11. M. Meyer, A. Philipp, R. Oskuee, C. Schmidt and E. Wagner, J. Am. Chem. Soc., 2008, 130, 3272-3273.

12. D. Weerakkody, A. Moshnikova, M. S. Thakur, V. Moshnikova, J. Daniels, D. M. Engelman, O. A. Andreev and Y. K. Reshetnyak, Proc. Natl. Acad. Sci. U. S. A., 2013, 110, 5834-5839.

13. L. Yao, J. Daniels, A. Moshnikova, S. Kuznetsov, A. Ahmed, D. M. Engelman, Y. K. Reshetnyak and O. A. Andreev, Proc. Natl. Acad. Sci. U. S. A., 2013, 110, 465-470.

14. Y. Li, W. Xiao, K. Xiao, L. Berti, J. Luo, H. P. Tseng, G. Fung and K. S. Lam, Angew. Chem. Int. Ed., 2012, 51, 2864-2869.

15. W. Chen, Y. Cheng and B. Wang, Angew. Chem. Int. Ed., 2012, 51, 5293-5295.

16. J. Ko, K. Park, Y. S. Kim, M. S. Kim, J. K. Han, K. Kim, R. W. Park, I. S. Kim, H. K. Song, D. S. Lee and I. C. Kwon, *J. Control. Release*, 2007, **123**, 109-115.

17. K. E. Broaders, S. J. Pastine, S. Grandhe and J. M. Frechet, Chem. Commun., 2011, 47, 665-667.

18. E. R. Gillies, T. B. Jonsson and J. M. Frechet, J. Am. Chem. Soc., 2004, 126, 11936-11943.

19. E. R. Gillies and J. M. Frechet, Bioconjugate Chem., 2005, 16, 361-368.

20. K. A. Sarosiek, L. E. Cavallin, S. Bhatt, N. L. Toomey, Y. Natkunam, W. Blasini, A. J. Gentles, J. C. Ramos, E. A. Mesri and I. S. Lossos, Proc. Natl. Acad. Sci. U. S. A., 2010, 107, 13069-13074.

21. A. Swami, M. R. Reagan, P. Basto, Y. Mishima, N. Kamaly, S. Glavey, S. Zhang, M. Moschetta, D. Seevaratnam, Y. Zhang, J. Liu, M. Memarzadeh, J. Wu, S. Manier, J. Shi, N. Bertrand, Z. N. Lu, K. Nagano, R. Baron, A. Sacco, A. M. Roccaro, O. C. Farokhzad and I. M. Ghobrial, Proc. Natl. Acad. Sci. U. S. A., 2014, 111, 10287-10292.

22. D. Schiff, P. Y. Wen and M. J. van den Bent, Nat. Rev. Clin. Oncol., 2009, 6, 596-603.

23. S. Grant, Blood, 2014, 123, 2910-2912.

24. J. Shen, G. Song, M. An, X. Li, N. Wu, K. Ruan, J. Hu and R. Hu, Biomaterials, 2014, 35, 316-326.

25. S. I. Thamake, S. L. Raut, Z. Gryczynski, A. P. Ranjan and J. K. Vishwanatha, Biomaterials, 2012, 33, 7164-7173.

26. J. D. Ashley, J. F. Stefanick, V. A. Schroeder, M. A. Suckow, T. Kiziltepe and B. Bilgicer, J. Med. Chem., 2014, 57, 5282-5292.

27. J. Su, F. Chen, V. L. Cryns and P. B. Messersmith, J. Am. Chem. Soc., 2011, 133, 11850-11853.

28. S. H. Wu, R. G. Qi, H. H. Kuang, Y. Wei, X. B. Jing, F. B. Meng and Y. B. Huang, ChemPlusChem, 2013, 78, 175-184.

29. S. Deshayes, H. Cabral, T. Ishii, Y. Miura, S. Kobayashi, T. Yamashita, A. Matsumoto, Y. Miyahara, N. Nishiyama and K. Kataoka, J. Am. Chem. Soc., 2013, 135, 15501-15507.

30. L. He, D. E. Fullenkamp, J. G. Rivera and P. B. Messersmith, Chem. Commun., 2011, 47, 7497-7499.

31. D. A. Tomalia, Prog. Polym. Sci., 2005, 30, 294-324.

32. D. A. Tomalia, L. A. Reyna and S. Svenson, Biochem. Soc. Trans., 2007, 35, 61-67.

33. D. A. Tomalia, Nanomedicine, 2012, 7, 953-956.

34. S. Sevenson and D. A. Tomalia, Adv. Drug Deliver. Rev., 2012, 64, 102-115.

35. A. R. Menjoge, R. M. Kannan and D. A. Tomalia, Drug Discov. Today, 2010, 15, 171-185.

36. C. C. Lee, J. A. MacKay, J. M. Frechet and F. C. Szoka, Nat. Biotechnol., 2005, 23, 1517-1526.

37. A. P. Goodwin, S. S. Lam and J. M. Frechet, J. Am. Chem. Soc., 2007, 129, 6994-6995.

38. A. Almutairi, R. Rossin, M. Shokeen, A. Hagooly, A. Ananth, B. Capoccia, S. Guillaudeu, D. Abendschein, C. J. Anderson, M. J. Welch and J. M. Frechet, Proc. Natl. Acad. Sci. U. S. A., 2009, 106, 685-690.

39. C. C. Lee, E. R. Gillies, M. E. Fox, S. J. Guillaudeu, J. M. Frechet, E. E. Dy and F. C. Szoka, Proc. Natl. Acad. Sci. U. S. A., 2006, 103, 16649-16654.

40. R. M. Kannan, E. Nance, S. Kannan and D. A. Tomalia, J. Intern. Med., 2014, 276, 579-617.

41. M. Wang, H. Liu, L. Li and Y. Cheng, Nat. Commun., 2014, 5, 3053.

42. L. Zhao, Q. Wu, Y. Cheng, J. Zhang, J. Wu and T. Xu, J. Am. Chem. Soc., 2010, 132, 13182-13184.

43. J. Hu, T. Xu and Y. Cheng, Chem. Rev., 2012, 112, 3856-3891.

44. X. Wang, X. Cai, J. Hu, N. Shao, F. Wang, Q. Zhang, J. Xiao and Y. Cheng, J. Am. Chem. Soc., 2013, 135, 9805-9810.

45. J. Hu, Y. Su, H. Zhang, T. Xu and Y. Cheng, Biomaterials, 2011, 32, 9950-9959.

44x44mm (300 x 300 DPI)